1

Graph Signal Processing in Wireless Sensor Networks

Gal Morgenstern[1], Lital Dabush[1], Morad Halihal[1], Tirza Routtenberg[1,2], and H. Vincent Poor[2]

[1] *School of ECE, Ben-Gurion University of the Negev, Beer-Sheva, Israel*
[2] *ECE Department, Princeton University, Princeton, NJ, USA*

1.1 Introduction

Wireless Sensor Networks (WSNs) have become central to modern data acquisition tasks, facilitating data gathering through interconnected sensor nodes [Akyildiz et al., 2002; Kandris et al., 2020]. Data originating from WSNs are usually distributed nonuniformly in space and time, which differs from regular-domain signals such as digital images and discrete-time sequences. Furthermore, WSNs are often implemented in applications that are characterized by complex and nonlinear models [He et al., 2004; Werner-Allen et al., 2006; Kim et al., 2019]. The processing of signals in WSNs is hence often intractable, especially for large networks, so it is crucial to develop advanced tools to model, process, and analyze them.

The field of graph signal processing (GSP) has gained considerable interest in the last decade due to the growing importance of networked data in various settings such as social, energy, transportation, sensor, and neural networks [Sandryhaila and Moura, 2013; Shuman et al., 2013; Ortega, 2022]. GSP theory expands concepts and techniques from traditional digital signal processing (DSP) to data indexed by graphs. GSP concepts include the graph Fourier transform (GFT), graph signal smoothness, graph filter design, and sampling and recovery of graph signals. Various GSP tools have been recruited to solve many fundamental engineering problems, such as signal denoising [Shuman et al., 2011], data reconstruction [Feng et al., 2021; Morgenstern and Routtenberg, 2024], node clustering [Sahai et al., 2012], consensus algorithms [Sandryhaila et al., 2014], and anomaly detection [Egilmez and Ortega, 2014]. Since these problems frequently

Wireless Sensor Networks in Smart Environments: Enabling Digitalization from Fundamentals to Advanced Solutions, First Edition. Edited by Domenico Ciuonzo and Pierluigi Salvo Rossi.

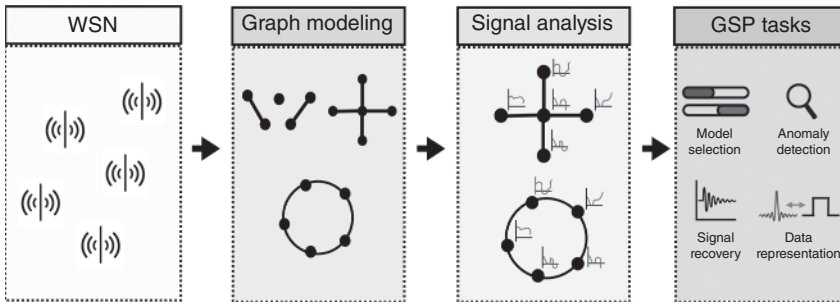

Figure 1.1 Overview of Chapter 1: end-to-end approach for processing networked signals using GSP tools in WSN applications. The approach comprises of sensor readings, graph modeling and signal analysis options, and the application of GSP tools to the acquired data.

feature in WSN data-processing tasks, the utilization of GSP tools in this context is particularly efficacious and could mark a significant shift in the methodologies and approaches employed in this sphere.

This chapter presents an end-to-end approach for processing WSN signals with GSP tools (see Figure 1.1). First, we introduce GSP-based models for WSNs as undirected weighted graphs in Section 1.2. Fundamental GSP concepts, including the graph Laplacian matrix, graph signal smoothness, and the graph spectrum, are then introduced in Section 1.3. Additionally, the chapter discusses the concept of graph signal smoothness validation in Section 1.4, which enables analyzing the signal with respect to (w.r.t.) the underlying graph. Next, based on the smoothness assumption, methods for graph signal recovery and anomaly detection are proposed in Sections 1.5 and 1.6, respectively. Utilizing the graph signal properties, we then present approaches to discover the underlying network structure. Finally, concluding remarks and future directions are given in Section 1.8.

1.2 Graph Models for WSNs

Graph theory enables the creation of intricate models that can effectively represent various types of relationships. In this context, we model WSNs as undirected weighted graphs. This approach is inherently intuitive, given that WSN deployments typically feature sensor nodes interconnected by communication links that are easily represented by graph structures. Consequently, this modeling approach enables the application of GSP tools in WSNs.

The graphical representation should capture the inherent spatial and functional relationships among sensor nodes and facilitate the translation of complex WSN

data into an analyzable graph format. Different models can be considered to this end. This section outlines the general elements of the WSN in graph terms and introduces three optional graph models [Egilmez and Ortega, 2014]: the distance-based model, the correlation-based model, and the hybrid distance and correlation-based model. These perspectives provide a nuanced understanding of the diverse ways in which graph theory can be applied to WSN data.

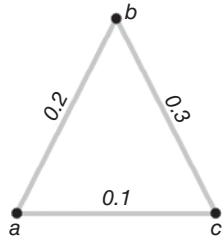

Figure 1.2
Illustration of an undirected graph with 3 nodes, $\mathcal{M} = \{a, b, c\}$, the edge set, $\xi = \{(a, b), (a, c), (b, c)\}$, and the edge weights, $w_{a,b} = 0.2$, $w_{a,c} = 0.1$, and $w_{b,c} = 0.3$.

We consider a WSN with $|\mathcal{M}|$ sensors, where each sensor measures a specific attribute. The underlying relation between the measured entities can be modeled by an undirected and weighted graph $\mathcal{G} = \{\mathcal{M}, \xi\}$, which consists of a set of nodes $\mathcal{M} = \{1, \dots, |\mathcal{M}|\}$ and a set of edges ξ. A positive edge weight between nodes k and m, $w_{k,m} > 0$, indicates that the nodes are connected, that is, $(k, m) \in \xi$, and quantifies the similarity between these nodes. Conversely, we define $w_{k,m} = 0$ if the nodes are not connected, that is, $(k, m) \notin \xi$. We assume that the graph is connected, the edge weights are positive, and no more than one edge can connect any pair of nodes, as illustrated in Figure 1.2.

In all the models below, the node set $\mathcal{M}$ is considered to be fixed. Thus, the graph model is equivalently determined by the graph adjacency matrix $\boldsymbol{W}$, defined by

$$W_{k,m} = \begin{cases} w_{k,m} & (k, m) \in \xi \\ 0 & \text{otherwise} \end{cases} \qquad k, m = 1, \dots, |\mathcal{M}| \,. \tag{1.1}$$

Hence, the adjacency matrix enables a matrix representation of the graph, which is often used for the design and formulation of graph models. In the following, we introduce different graph-based models appropriate for WSNs by defining their adjacency matrices.

1.2.1 Distance-Based Model

In this model, we consider the case where the locations of the sensors are known. This is often the case when the system sensors obtain a Global Positioning System (GPS) tag, or, in static systems. The underlying assumption in this model is that the distance between the sensors also defines the relation between the entities. For example, in environmental monitoring systems, it is a fair assumption that measurements gathered from closely positioned sensors will exhibit similar values [Sandryhaila and Moura, 2013]. By denoting $D(k, m)$ as the 2D-Euclidean distance

between the locations of the sensors at nodes k and m, we define the distance-based adjacency matrix, $\boldsymbol{W}^{(d)}$ elementwisely by [Shuman et al., 2013]:

$$W_{k,m}^{(d)} = \begin{cases} e^{\frac{-D(k,m)^2}{\Delta_d^2}} & D(k,m) \leq \gamma_d \\ 0 & \text{otherwise,} \end{cases} \tag{1.2}$$

where Δ_d determines the exponential decay rate, and γ_d is the threshold determining the graph connectivity. It can be seen that selecting a low value for γ_d results in a low number of edges, i.e. with a sparse graph.

The distance-based modeling proposed in (1.2) is illustrated in Figure 1.3. It is important to highlight that (1.2) can be readily generalized for 3D-Euclidean distance and for alternative distance metrics, such as the Manhattan distance [Cardei et al., 2008].

1.2.2 Correlation-Based Model

In this model, we consider the case where the underlying relation between the system nodes can be characterized due to their spatial and/or temporal correlations [Pradhan et al., 2002; Vuran and Akyildiz, 2006]. By defining $\rho(k,m)$ as the correlation coefficient between the entities measured by the sensors at nodes k and m, we define the correlation-based adjacency matrix, $\boldsymbol{W}^{(c)}$ elementwisely by

$$W_{k,m}^{(c)} = \begin{cases} |\rho(k,m)| & |\rho(k,m)| \geq \gamma_c \\ 0 & \text{otherwise,} \end{cases} \tag{1.3}$$

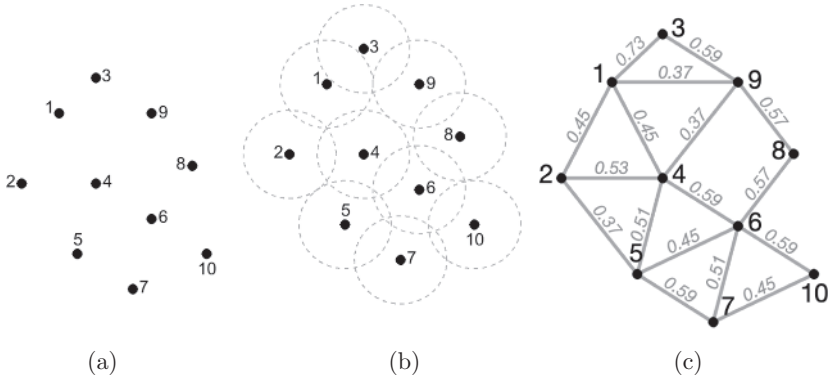

Figure 1.3 Illustration of the distance-based model: (a) system sensors: sensor network depicted in a 2D-Euclidean space. (b) Sensor-centered circles of radius $\gamma_d = 2.2$, each sensor is associated with a circle of radius $\gamma_d/2$. (c) The resulting distance-based graph, where nodes are connected by an edge if the spheres corresponding to two (or more) circles intersect, indicating that the distance between vertices is smaller than γ_d. The parameter Δ_d has been set to $\Delta_d = \gamma_d = 2.2$.

where γ_c is the threshold determining the graph connectivity. In a similar manner to in (1.2), selecting a high value of γ_c in (1.3) will result in a sparse graph.

Hybrid models that take into account both the correlation between the application entities and the geometric positions of the sensors can also be considered. For instance, here we define the hybrid-distance- and correlation-based adjacency matrix, $\boldsymbol{W}^{(b)}$ elementwisely by

$$W_{k,m}^{(b)} = \begin{cases} e^{-\frac{D(k,m)^2}{\Delta_d^2}} e^{-\frac{(1-|\rho(k,m)|)^2}{\Delta_c^2}} & |\rho(k,m)| \geq \gamma_c \text{ and } D(k,m) \leq \gamma_d \\ 0 & \text{otherwise,} \end{cases} \tag{1.4}$$

where $D(k,m)$ and $\rho(k,m)$ are the 2D-Euclidean distance and the correlation coefficient between nodes k and m, respectively. The parameters Δ_c and Δ_d determine the exponential decay rate for each of the exponents, and the thresholds γ_d and γ_c determine the graph connectivity. It can be seen that in order for two nodes to be connected, they must be sufficiently correlated, i.e. $|\rho(k,m)| \geq \gamma_c$, and obtain a short enough distance, i.e. $D(k,m) \leq \gamma_d$. Additionally, the parameters Δ_c and Δ_d also determine which of the properties is more dominant in the relation quantified by the edge weight.

1.2.3 Alternative Models

It should be noted that the modeling of the underlying graph in WSN applications is not limited to the models described above and can be specified depending on the application. For example, in WSNs deployed in power systems [Tariq and Poor, 2016], the underlying graph may naturally emerge from the physical interactions of the system. Moreover, additional elements in WSNs, such as sink nodes and communication links, can also be considered as part of the modeling [Schizas et al., 2008]. Thus, certain scenarios may favor a communication-based graph over a distance-based one, emphasizing communication paths and accommodating the representation of communication losses due to obstacles. Some additional graph models may also be considered: (i) a grid-based model for structured layouts, where nodes are connected if they share an edge in the grid [Servetto and Barrenechea, 2002] (this model is suitable for applications like agricultural monitoring [Díaz et al., 2011]); (ii) a random geometric graph model (this is realistic for scenarios where sensor nodes are deployed randomly and communication is confined to nearby nodes [Ramamoorthy et al., 2005]); (iii) a hierarchical/tree topology (this is beneficial for efficient data aggregation and transmission to a central point [Hasheminejad and Barati, 2021]); and (iv) a mesh topology, where each sensor node serves as a router, enabling multi-hop communication and offering redundancy and multiple paths for enhanced network reliability (this is particularly suitable in applications where robustness and fault tolerance are critical [Nurlan et al., 2021]).

1.3 Concepts in GSP

In WSNs, sensor measurements can be represented as graph signals defined as

$$\mathbf{x}: \mathcal{M} \to \mathbb{R}^{|\mathcal{M}|}. \tag{1.5}$$

Each signal element in (1.5) is a real-valued parameter that is associated with a single node of the graph. This definition can be extended to more complicated scenarios, including multidimensional vectors at each node and signals incorporating missing measurements.

A graph shift operator (GSO), $\mathbf{S}$, operates on graph signals, similar to how time shift operates on time series in DSP. However, while time shift adjusts the position of signal values along the time axis, a graph shift redistributes signal values based on the structure of the underlying graph. The GSO, $\mathbf{S}$, is an $|\mathcal{M}| \times |\mathcal{M}|$ matrix with entries that satisfy

$$S_{k,m} = 0, \quad \text{if } k \neq m \quad \text{and} \quad (k,m) \notin \xi, \ \forall k, m \in \mathcal{M}. \tag{1.6}$$

Consequently, the GSO defines a local operator that, when applied on a graph signal, $\mathbf{x}$, results in

$$[\mathbf{S}\mathbf{x}]_k = S_{k,k}x_k + \sum_{m:(k,m)\in\xi} S_{k,m}x_m. \tag{1.7}$$

That is, the signal value x_k at node k is replaced with a linear combination of values at the node itself and the neighbors of node k.

GSP tools can be developed for various GSOs such as the adjacency matrix in (1.1). For the sake of simplicity, the tools presented in this chapter are based on the specific GSO of the graph Laplacian matrix, $\mathbf{L}$. The elements of the matrix $\mathbf{L}$ are defined as

$$L_{k,m} = \begin{cases} \sum_{(k,j)\in\xi} w_{k,j} & k = m \\ -w_{k,m} & (k,m) \in \xi \\ 0 & \text{otherwise} \end{cases} \qquad k, m = 1, \ldots, |\mathcal{M}|. \tag{1.8}$$

Similar to the adjacency matrix in (1.1), the graph Laplacian matrix fully captures the graph structure. The relation between those matrices is given by

$$\mathbf{L} = \text{diag}(\mathbf{1}^T\mathbf{W}) - \mathbf{W}, \tag{1.9}$$

where $\text{diag}(\mathbf{1}^T\mathbf{W})$ is a diagonal matrix whose (k,k)th entry is $\sum_{m=1}^{|\mathcal{M}|} W_{k,m}$, and $\mathbf{1}$ is the all-one vector.

1.3.1 Graph Spectrum

The graph Laplacian matrix of the graph $\mathcal{G}$, which is defined in (1.8), is a real, symmetric, and positive semidefinite matrix. Thus, its singular value decomposition (SVD) is given by

$$\mathbf{L} = \mathbf{V}\,\mathrm{diag}(\lambda)\mathbf{V}^T, \tag{1.10}$$

where the columns of $\mathbf{V}$, $\{\mathbf{V}_i\}_{i\in\mathcal{M}}$, are the eigenvectors of $\mathbf{L}$ and thus satisfy $\mathbf{V}^T = \mathbf{V}^{-1}$. The diagonal matrix $\mathrm{diag}(\lambda) \in \mathbb{R}^{|\mathcal{M}|\times|\mathcal{M}|}$ consists of the eigenvalues of $\mathbf{L}$, $\lambda_1, \dots, \lambda_{|\mathcal{M}|}$, which satisfy $0 = \lambda_1 \le \lambda_2 \le \cdots \le \lambda_{|\mathcal{M}|}$. Additionally, under the assumption that the graph is connected, it can be verified that the eigenvalues satisfy $\lambda_k > 0, k = 2, \dots, |\mathcal{M}|$.

The SVD of the graph Laplacian matrix enables a definition for the graph spectrum of $\mathcal{G}$. Specifically, the eigenvalues, $\lambda_1, \dots, \lambda_{|\mathcal{M}|}$, are interpreted as graph frequencies with the eigenvectors in $\mathbf{V}$ as their corresponding graph frequency components. Using this interpretation, we can represent the graph signal in (1.5) in the graph frequency domain by

$$(a)\ \tilde{\mathbf{x}} = \mathbf{V}^T\mathbf{x},\ (b)\ \mathbf{x} = \mathbf{V}\tilde{\mathbf{x}}, \tag{1.11}$$

where (a) represents the GFT of the vector $\mathbf{x}$ and (b) represents the inverse GFT of $\tilde{\mathbf{x}}$.

1.3.2 Graph Signal Properties

A central focus of GSP is analyzing the graph signal defined in (1.5) and identifying its unique properties w.r.t. the underlying graph. In this context, an important property in GSP is graph signal smoothness, where a graph signal is considered to be smooth when its values exhibit moderate variations across the graph, i.e. signal elements have similar values at neighboring nodes. The graph total variation (GTV) is a key measure of smoothness [Shuman et al., 2013], which is defined in the node domain by

$$TV^{\mathcal{G}}(\mathbf{x}) \triangleq \mathbf{x}^T\mathbf{L}\mathbf{x} = \frac{1}{2}\sum_{k=1}^{|\mathcal{M}|}\sum_{m=1}^{|\mathcal{M}|} w_{k,m}\left(x_k - x_m\right)^2. \tag{1.12}$$

By substituting (1.10) and (1.11) in (1.12), we obtain the GTV definition in the graph frequency domain:

$$TV^{\mathcal{G}}(\mathbf{x}) = \mathbf{x}^T\mathbf{V}\mathrm{diag}(\lambda)\mathbf{V}^T\mathbf{x} = \tilde{\mathbf{x}}^T\ \mathrm{diag}(\lambda)\tilde{\mathbf{x}} = \sum_{k=1}^{|\mathcal{M}|}\lambda_k\tilde{\mathbf{x}}_k^2. \tag{1.13}$$

According to (1.12), a graph signal $\mathbf{x}$ is smooth if its GTV, $TV^{\mathcal{G}}(\mathbf{x})$, is small in terms of the specific application. It can be seen that in order for a graph signal to be

considered smooth, its elements in connected nodes need to have similar values (according to the right-hand side (r.h.s.) of (1.12)), and its graph spectrum needs to be concentrated in the small eigenvalues region (according to the r.h.s. of (1.13)). The assessment of graph variation can also be formulated using alternative vector norms, such as other ℓ_p norms [Chen et al., 2015a].

An example of a smooth graph signal is a low-frequency bandlimited graph signal, defined as follows.

Definition 1.1 ***(Bandlimited graph signal)*** A graph signal, $\mathbf{x}$, is ideal β-bandlimited in the graph frequency domain w.r.t. the GFT basis $\mathbf{V}$ if

$$\tilde{x}_k = 0, \;\; k = \beta + 1, \ldots, |\mathcal{M}|, \tag{1.14}$$

where the parameter β is referred to as the cutoff graph frequency.

Definition 1.1 implies sparsity in the signal's representation in the spectral, graph frequency domain. Intuitively, similar to bandlimited DSP signals, which are characterized by a low variation over consecutive time slots, a graph-bandlimited signal is expected to obtain a low GTV.

In Figure 1.4, we present the first, third, fifth, and eight eigenvectors of the graph Laplacian matrix associated with the graph from Figure 1.3c, to illustrate the concept of graph signal smoothness. It can be seen that the eigenvectors display an increasing variation w.r.t. the graph as the eigenvalue (graph frequency) increases.

1.3.3 Graph Filters

Filtering constitutes a fundamental concept in GSP applications, similar to in DSP. A graph filter is a function $h(\cdot)$ applied to a GSO, which is associated with the underlying graph. By selecting the GSO as the graph Laplacian matrix, $\mathbf{L}$, we present the following definition for graph filters based on the SVD in (1.10).

Definition 1.2 ***(Graph filters)*** For a given graph associated with the graph Laplacian matrix $\mathbf{L}$, a graph filter $h(\mathbf{L})$ is an $|\mathcal{M}| \times |\mathcal{M}|$ matrix given by

$$h(\mathbf{L}) = \mathbf{V}\text{diag}(h(\lambda))\mathbf{V}^T, \tag{1.15}$$

where $h(\lambda) \triangleq (h(\lambda_1), \ldots, h(\lambda_{|\mathcal{M}|}))$ is the graph frequency response and corresponds to the graph frequencies λ_k, $k = 1, \ldots, |\mathcal{M}|$ defined in (1.10). Moreover, if the eigenvalues are not distinct, then $h(\lambda_k) = h(\lambda_m)$ for any k and m that satisfy $\lambda_m = \lambda_k$ [Ortega, 2022].

The output of the graph filter, provided with the input signal $\mathbf{x}$, i.e.

$$\mathbf{y} = h(\mathbf{L})\mathbf{x}, \tag{1.16}$$

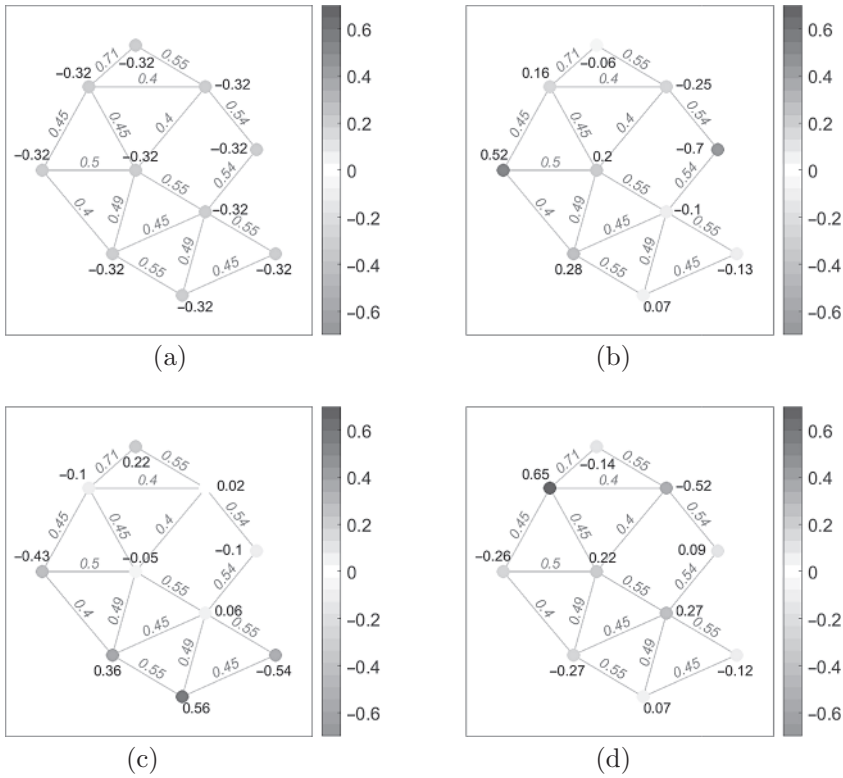

Figure 1.4 Example of Four eigenvectors of the graph Laplacian matrix associated with the graph in Figure 1.3. Each eigenvector is a graph signal, and the shading (and the number) at each node represents the signal value at the node. (a) $\lambda_1 = 0$, (b) $\lambda_3 = 0.81$, (c) $\lambda_5 = 1.52$, and (d) $\lambda_8 = 2.51$.

is also a graph signal, as defined in (1.5). Moreover, as shown in the following theorem, in the graph spectral domain, the output signal is the result of a Hadamart product (elementwise product) between the input signal and the graph frequency response. A block diagram of this filtering process is presented in Figure 1.5.

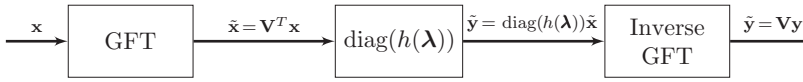

Figure 1.5 Block diagram illustrating the filtering of a graph signal **x** by the graph filter in (1.15).

Theorem 1.1 The graph spectral representation of the filtered signal satisfies

$$\tilde{\mathbf{y}} = \text{diag}(h(\lambda))\tilde{\mathbf{x}} \tag{1.17}$$

if and only if $h(\mathbf{L})$ is defined by (1.15).

Proof: ($\rightarrow$) By multiplying $\mathbf{V}$ on both sides of (1.17) and using the definitions of the GFT and the inverse GFT from (1.11), we obtain

$$\mathbf{y} = \mathbf{V}\tilde{\mathbf{y}} = \mathbf{V}\text{diag}(h(\lambda))\tilde{\mathbf{x}} = \mathbf{V}\text{diag}(h(\lambda))\mathbf{V}^T\mathbf{x}.$$

Hence, the graph filter in this case is defined by (1.15).

($\leftarrow$) By substituting (1.15) in the definition of the inverse GFT from (1.11), we obtain

$$\tilde{\mathbf{y}} = \mathbf{V}^T\mathbf{y} = \mathbf{V}^T\mathbf{V}\text{diag}(h(\lambda))\mathbf{V}^T\mathbf{x} = \text{diag}(h(\lambda))\tilde{\mathbf{x}}. \tag{1.18}$$

From Theorem 1.1, we observe that filtering a signal with the graph filter in (1.15) is equivalent in the graph frequency domain to multiplying the signal's spectrum by the frequency response of the filter. Thus, (1.15) can be perceived as an extension of the *convolution theorem* from DSP to graphs [Shuman et al., 2013]. Consequently, in a similar manner to DSP, the graph filter in (1.15) can be categorized based on its filter frequency response, e.g. as low-pass, band-pass, high-pass, or all-pass [Sandryhaila and Moura, 2014].

The following definition and theorem present an alternative representation of the graph filter in (1.15). In this representation, the graph filter is defined as a polynomial of the graph Laplacian matrix.

Definition 1.3 ***(Graph filters – alternative representation)*** For a given graph associated with the graph Laplacian matrix $\mathbf{L}$, a shift-invariant graph filter $h(\mathbf{L})$ is an $N \times N$ matrix that can be written as a polynomial of $\mathbf{L}$:

$$h(\mathbf{L}) = p(\mathbf{L}) = \sum_{j=0}^{J} a_j \mathbf{L}^j, \tag{1.19}$$

where $\mathbf{L}^0 = \mathbf{I}$ and the scalars $\{a_j\}_j$ are the polynomial coefficients.

Theorem 1.2 Any shift-invariant graph filter, defined as in (1.19), can be defined as the graph filter in (1.15).

Proof: The proof can be found in Page 86 in Ortega [2022].

The shift-invariant graph filter in (1.19) is a local operator. That is, the filter output at node k, y_k, is a linear combination of the input signal at nodes with a geodesic distance smaller than or equal to J from node k. This filter is a generalization of the

conventional DSP shift-invariant filter, applied to graph signals. Moreover, analogously to DSP shift-invariant filters, matrix multiplication between shift-invariant graph filters is commutative.

It is noted that the graph filters presented in this chapter can be alternatively defined using other GSOs instead of the graph Laplacian matrix [Sandryhaila et al., 2014].

1.4 GSP-Based Smoothness Validation for WSN Signals

Graph signals obtained from WSN data exhibit smoothness, i.e. a low GTV, as defined in (1.12). This observation seems intuitive when considering the correlation-based model in Section 1.2.2 and may also hold true for the distance-based model in Section 1.2.1, given that WSN data often exhibit spatial similarity features [Pattem et al., 2008; Kong et al., 2013]. Graph signal smoothness is the basis for a variety of GSP approaches that can be utilized for WSN applications, including signal recovery (see Section 1.5) and anomaly detection (see Section 1.6). Therefore, in these applications, assessing the smoothness level of system signals w.r.t. the underlying graph is expected to provide insights that can enhance the application performance.

1.4.1 Smooth Graph Filters

A smooth graph filter is a special case of the graph filter defined in (1.15), in which the output signal $\mathbf{y}$ from (1.16) has a low GTV as defined in (1.12). The following definition gives a mathematical expression for this concept [Shaked and Routtenberg, 2021; Dabush and Routtenberg, 2024].

Definition 1.4 ***(Smooth graph filter)*** Let the elements of the input graph signal, $\mathbf{x}$, be independent and identically distributed (i.i.d.) zero-mean random variables. Additionally, denote $\mathbf{y}$ as the output of the graph filter. Then, $h(\cdot)$ in (1.15) is a smooth graph filter if

$$r \triangleq \frac{\mathrm{E}[\|\mathbf{x}\|^2]}{\mathrm{E}[\|\mathbf{y}\|^2]} \times \frac{\mathrm{E}[\mathbf{y}^T\mathbf{L}\mathbf{y}]}{\mathrm{E}[\mathbf{x}^T\mathbf{L}\mathbf{x}]} < 1. \tag{1.20}$$

It can be seen that Definition 1.4 is based on the GTV. In [Dabush and Routtenberg, 2023], it is shown that r can be written in the graph frequency domain as

$$r = \lambda_{avg}^{-1} \times \frac{\sum_{k=1}^{|\mathcal{M}|} \lambda_k h^2(\lambda_k)}{\sum_{k=1}^{|\mathcal{M}|} h^2(\lambda_k)} < 1, \quad \text{where} \quad \lambda_{avg} \triangleq \frac{1}{|\mathcal{M}|}\sum_{k=1}^{|\mathcal{M}|}\lambda_k. \tag{1.21}$$

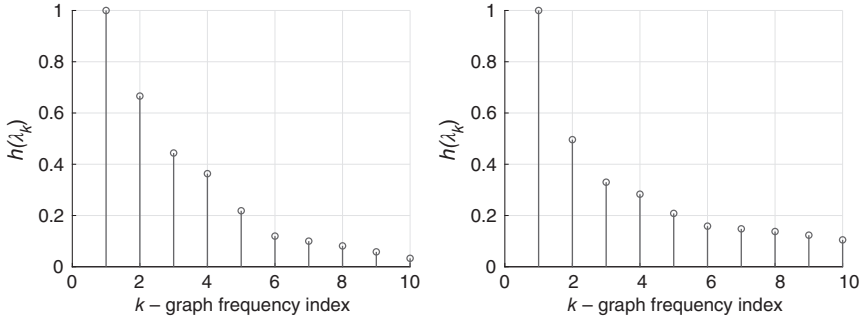

Figure 1.6 Examples of smooth graph filters. (a) Heat diffusion Kernel filter and (b) Laplacian (Tikhonov) filter.

Thus, if the energy of the frequency response is uniformly distributed across all graph frequencies, the ratio will be 1, indicating that the graph filter is not smooth. If the energy is biased toward low graph frequencies, the ratio will be lower than 1, indicating that the graph filter is smooth.

In Figure 1.6, we present two smooth graph filters [Isufi et al., 2024]: (i) the heat diffusion kernel filter, $h(\lambda_k) = \exp\{-\lambda_k\}$, $k = 1, \dots, |\mathcal{M}|$ and (ii) the Laplacian (Tikhonov) filter, $h(\lambda_k) = 1/(1 + 2.5\lambda_k)$, $k = 1, \dots, |\mathcal{M}|$. It can be seen that both filters are graph low-pass filters (GLPFs) that preserve the energy in the lower graph frequencies of the input signal, while reducing the energy of the signal at the higher graph frequency regime. Thus, they are smooth graph filters (1.21).

In Figure 1.7 we compare the input signal $\mathbf{x}$, which is drawn from the Gaussian distribution $\mathcal{N}(\mathbf{0}, \mathbf{I})$, with the output $\mathbf{y}$, which is filtered by the heat-diffusion-kernel GLPF. As expected, the output signal exhibits smoother variation over the graph in the vertex domain. In addition, it can be seen that the higher graph frequencies of the input signal have been attenuated.

We conclude our discussion on smooth graph filters with the following two remarks.

Remark 1.1 An alternative definition that evaluates whether a graph filter can be considered as a graph low-pass (GLP) filter is described in Definition 1 in Ramakrishna et al. [2020].

Remark 1.2 Modeling graph signals as outputs of graph filters is common practice for signal analysis widely used in GSP and graph neural networks (GNNs) [Schultz et al., 2021; He and Wai, 2022; Kroizer et al., 2022]. Specifically, smooth graph signals are often modeled as the output of smooth graph filters, where the input is a white Gaussian noise vector [Kalofolias, 2016; Dong et al., 2020].

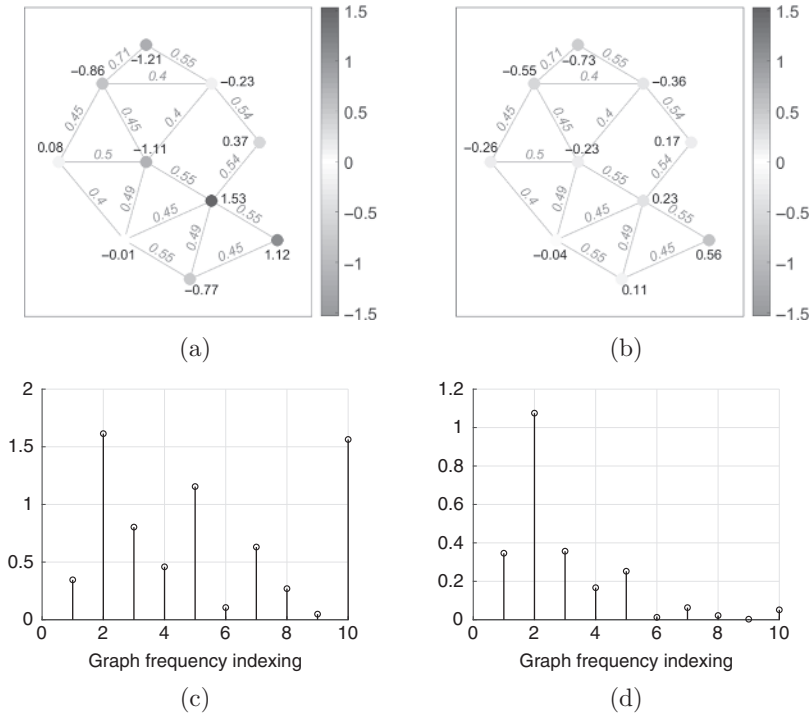

Figure 1.7 Example: comparison between the input signal $\mathbf{x}$, which is drawn from the Gaussian distribution $\mathcal{N}(\mathbf{0}, \mathbf{I})$, and the output $\mathbf{y}$, which is filtered by the heat-diffusion-kernel GLPF $h(\lambda_k) = \exp\{-\lambda_k\}$, $k = 1, \ldots, |\mathcal{M}|$. (a) Input: $\mathbf{x}$, $TV^{\mathcal{G}}(\mathbf{x}) = 13.2942$, (b) Output: $\mathbf{y}$, $TV^{\mathcal{G}}(\mathbf{y}) = 0.7179$, (c) $\tilde{\mathbf{x}} = \mathbf{V}^T\mathbf{x}$, and (d) $\tilde{\mathbf{y}} = \mathbf{V}^T(\mathbf{y})$.

1.4.2 Semi-parametric Graph Signal Smoothness Detector

In this section, our goal is to determine whether a sequence of signals $\{\mathbf{y}[n]\}_{n=1}^N$ are smooth graph signals. Based on Remark 1.2, the signals $\{\mathbf{y}[n]\}_{n=1}^N$ are modeled as the outputs of a linear graph filter, as defined in (1.16):

$$\mathbf{y}[n] = h(\mathbf{L})\mathbf{x}[n], \qquad n = 1, \ldots, N, \tag{1.22}$$

where $\{\mathbf{x}[n]\}_{n=1}^N$ are i.i.d. Gaussian random vectors, $\mathbf{x}[n] \sim \mathcal{N}(\mathbf{0}, \sigma^2\mathbf{I})$ and $\sigma^2 = 1$. The smoothness validation problem is formulated as the following composite hypothesis testing problem:

$$\begin{cases} \mathcal{H}_0: \ h(\mathbf{L}) \text{ is a smooth graph filter} \\ \mathcal{H}_1: \ h(\mathbf{L}) \text{ is a non-smooth graph filter.} \end{cases} \tag{1.23}$$

It should be noted that since we are dealing with real data from WSNs, we cannot presume knowledge of the graph filter, $h(\mathbf{L})$. Thus, as an integral part of the

detection approach, we employ a data-driven approach to the estimation of the graph filter. For the sake of simplicity, we assume that $h(\mathbf{L})$ is a non-singular matrix, and all the eigenvalues of $\mathbf{L}$ are distinct. These assumptions are chosen for simplicity, and the proposed detector can be developed without them, as shown in [Dabush and Routtenberg, 2023].

In order to solve the composite hypothesis testing problem in (1.23), we estimate the graph filter frequency response, i.e. $\{h^2(\lambda_k),\, k = 1, \ldots, |\mathcal{M}|\}$, from the measurements, and use the condition in (1.21) in order to determine whether the graph filter is smooth.

The log-likelihood function of the measurement model from (1.22) parametrized by $\{h^2(\lambda_k) \mid k = 1, \ldots, |\mathcal{M}|\}$ after removing constant terms is

$$\log f(\mathbf{y}; h^2(\mathbf{L})) \propto \frac{N}{2} \log(|h^2(\mathbf{L})|) - \frac{1}{2} \sum_{n=1}^{N} \mathbf{y}^T[n] (h^2(\mathbf{L}))^{-1} \mathbf{y}[n], \tag{1.24}$$

where $|\cdot|$ denotes the determinant of its argument matrix.

Based on (1.15), we replace $h(\mathbf{L})$ with its SVD, $\mathbf{V}\text{diag}(h(\lambda))\mathbf{V}^T$, in the log-likelihood in (1.24). Accordingly, the Maximum Likelihood (ML) estimator (see Chapter 7 in [Kay, 1993a]) is reduced to

$$\begin{aligned} \hat{h}^2(\lambda) &= \arg \max_{h^2(\lambda) \in \mathbb{R}^N} \log f(\mathbf{y}; h^2(\lambda)) \\ &= \arg \max_{h^2(\lambda) \in \mathbb{R}^N} \frac{N}{2} \log \left(|\mathbf{V} \big(\text{diag}(h^2(\lambda))\big)^{-1} \mathbf{V}^T| \right) \\ &\quad - \frac{1}{2} \sum_{n=1}^{N} \mathbf{y}^T[n] \mathbf{V} \left(\text{diag}(h^2(\lambda))^{-1} \right) \mathbf{V}^T \mathbf{y}[n], \end{aligned} \tag{1.25}$$

where $h(\lambda) = (h(\lambda_1), \ldots, h(\lambda_{|\mathcal{M}|}))$. By using the GFT definition in (1.11) and the fact that $\mathbf{V}$ is a unitary matrix, we can write (1.25) in the graph frequency domain as

$$\hat{h}^2(\lambda) = \arg \max_{h^2(\lambda) \in \mathbb{R}^N} \frac{N}{2} \sum_{k=1}^{|\mathcal{M}|} \log \left(\big(h^2(\lambda_k)\big)^{-1} \right) - \frac{1}{2} \sum_{k=1}^{|\mathcal{M}|} \big(h^2(\lambda_k)\big)^{-1} \sum_{n=1}^{N} \tilde{y}_k^2[n]. \tag{1.26}$$

By equating the derivative of the log-likelihood function from (1.26), w.r.t. each of the graph filter frequencies, $h^2(\lambda_k)$, $k = 1, \ldots, |\mathcal{M}|$, to zero, one obtains

$$\hat{h}^2(\lambda_k) = \frac{1}{N} \sum_{n=1}^{N} \tilde{y}_k^2[n], \quad k = 1, \ldots, |\mathcal{M}|. \tag{1.27}$$

By substituting (1.27) in the condition for smooth graph filters in (1.21), one obtains

$$\hat{r} = \lambda_{\text{avg}}^{-1} \frac{\sum_{k=1}^{|\mathcal{M}|} \sum_{n=1}^{N} \lambda_k \tilde{\mathbf{y}}_k^2[n]}{\sum_{k=1}^{|\mathcal{M}|} \sum_{n=1}^{N} \tilde{\mathbf{y}}_k^2[n]} < 1. \tag{1.28}$$

By replacing the order of summation in both the numerator and the denominator, substituting (1.13) in the numerator and (1.11) in the denominator, and using the unitary matrix property $\|\mathbf{V}\mathbf{y}\|^2 = \|\mathbf{y}\|^2$, one obtains

$$\hat{r} = \lambda_{avg}^{-1} \frac{\sum_{n=1}^{N} \mathbf{y}^T[n]\mathbf{L}\mathbf{y}[n]}{\sum_{n=1}^{N} \|\mathbf{y}[n]\|^2} < 1. \tag{1.29}$$

The detector in (1.29) is the sample mean of the GTV of the filtered signal $\mathbf{y}$, w.r.t. to the underlying graph, normalized by its sample variance and the average graph frequency λ_{avg}. Thus, the proposed detector can be interpreted as an empirical evaluation of the GTV of the output graph signal, $\mathbf{y}$.

1.5 GSP-Based Signal Recovery in WSN Models with Missing Data

Data loss is a frequent problem in WSNs that may be caused by a variety of factors such as noise, collisions, unreliable links, and damage. Consequently, many WSN applications operate under partial observation models [Kong et al., 2013]. Several signal reconstruction techniques have been developed to address this issue, including compressive-sensing-based methods [Kong et al., 2013], K-nearest neighbors-based methods [Pan and Li, 2010], and spatial–temporal imputation-based methods [Li and Parker, 2008]. In general, signal recovery from inaccessible and/or corrupted measurements requires additional knowledge of signal properties. To compensate for missing data over the graph, one can leverage the properties of graph signals that are often bandlimited or smooth graph signals [Chen et al., 2015a; Marques et al., 2015; Romero et al., 2016]. In this section, we consider the latter approach and utilize the graph signal smoothness of signals in WSN applications. It should be noted that the efficiency of the proposed methods is influenced by the graph signal smoothness level of the application's signals.

We consider the following observation model:

$$\mathbf{y} = \mathbf{\Phi}\mathbf{x} + \mathbf{n}, \tag{1.30}$$

where $\mathbf{\Phi} \in \mathbb{R}^{Q \times |\mathcal{M}|}$ represents a linear operation on the graph signal $\mathbf{x}$, and $\mathbf{n}$ is modeled by the Gaussian vector $\mathbf{n} \sim \mathcal{N}(\mathbf{0}, \mathbf{R}) \in \mathbb{R}^Q$. Furthermore, it is assumed

that the measurements in the set $\{Q \backslash \mathcal{S}\}$ are the measurements missing. Thus, the task is to recover the signal, $\mathbf{x}$, based on the missing data model

$$\mathbf{y}_{\mathcal{S}} = \mathbf{\Phi}_{\mathcal{S},\mathcal{M}}\mathbf{x} + \mathbf{n}_{\mathcal{S}}, \tag{1.31}$$

where $\mathbf{\Phi}_{\mathcal{S},\mathcal{M}}$ is the submatrix of $\mathbf{\Phi}$ that contains only the rows associated with the index set $\mathcal{S}$.

1.5.1 Signal Recovery Approaches

Approach 1. Weighted Least Squares (WLS): A common approach for estimating $\mathbf{x}$ based on the measurement model in (1.31) is by the WLS optimization problem:

$$\begin{aligned}\hat{\mathbf{x}}^{\text{WLS}} &= \arg\min_{\mathbf{x}\in\mathbb{R}^{|\mathcal{M}|}} (\mathbf{y}_{\mathcal{S}} - \mathbf{\Phi}_{\mathcal{S},\mathcal{M}}(\mathbf{L})\mathbf{x})^T\mathbf{R}^{-1}(\mathbf{y}_{\mathcal{S}} - \mathbf{\Phi}_{\mathcal{S},\mathcal{M}}(\mathbf{L})\mathbf{x}) \\ &= \left(\mathbf{\Phi}_{\mathcal{S},\mathcal{M}}(\mathbf{L})\right)^{\dagger}\mathbf{y}_{\mathcal{S}},\end{aligned} \tag{1.32}$$

where $(\cdot)^{\dagger}$ denotes the pseudo-inverse operator. However, this approach may not be suitable for the partial observation model in (1.31). Specifically, when the columns of $\mathbf{\Phi}_{\mathcal{S},\mathcal{M}}$ become linearly dependent, it is required to incorporate additional properties beyond the measurement model in (1.31) to achieve a unique estimator of $\mathbf{x}$.

Approach 2. WLS with GTV-based regularization: The recovery of smooth graph signals by incorporating regularization terms has been well-studied in the literature [Ortega et al., 2018; Puy and Pérez, 2018]. In particular, recovery with a regularization using the Laplacian quadratic form has been used in various applications including image processing, data classification, and supervised learning on graphs [Belkin et al., 2004; Wang and Zhang, 2006; Elmoataz et al., 2008; Cai et al., 2010; Zheng et al., 2010]. This approach involves incorporating a constraint on the GTV of the graph signal in the WLS problem in (1.32), which is formulated by

$$\begin{aligned}\hat{\mathbf{x}}^{\text{GSP-WLS}} = \arg\min_{\mathbf{x}\in\mathbb{R}^{|\mathcal{M}|}} &\left((\mathbf{y}_{\mathcal{S}} - \mathbf{\Phi}_{\mathcal{S},\mathcal{M}}(\mathbf{L})\mathbf{x})^T\mathbf{R}^{-1}(\mathbf{y}_{\mathcal{S}} - \mathbf{\Phi}_{\mathcal{S},\mathcal{M}}(\mathbf{L})\mathbf{x})\right) \\ &\text{such that } \mathbf{x}^T\mathbf{L}\mathbf{x} \le \varepsilon.\end{aligned} \tag{1.33}$$

The parameter ε and the efficiency of the GSP-WLS estimation depend on the smoothness properties of the signal that can be validated as discussed in Section 1.4.

By using the Karush–Kuhn–Tucker (KKT) conditions, the minimization problem in (1.33) can be replaced by the following regularized optimization problem:

$$\hat{\mathbf{x}}^{\text{GSP-WLS}} = \arg\min_{\mathbf{x}\in\mathbb{R}^{|\mathcal{M}|}} \left((\mathbf{y}_{\mathcal{S}} - \mathbf{\Phi}_{\mathcal{S},\mathcal{M}}\mathbf{x})^T\mathbf{R}^{-1}(\mathbf{y}_{\mathcal{S}} - \mathbf{\Phi}_{\mathcal{S},\mathcal{M}}\mathbf{x}) + \mu\,\mathbf{x}^T\mathbf{L}\mathbf{x}\right). \tag{1.34}$$

The term $\mathbf{x}^T\mathbf{L}\mathbf{x}$ is a regularization term that is based on the smoothness constraint from (1.33). The parameter $\mu \ge 0$ is a Lagrange multiplier, which is a tuning

parameter that replaces ε. The GSP-WLS estimator from (1.34) is obtained by equating the derivative of (1.34) w.r.t. $\mathbf{x}$ to zero, which results in [Wieringen, 2015]

$$\hat{\mathbf{x}}^{\text{GSP-WLS}} = \left(\mathbf{\Phi}_{S,\mathcal{M}}^T \mathbf{R}^{-1} \mathbf{\Phi}_{S,\mathcal{M}} + \mu \mathbf{L}\right)^{-1} \mathbf{\Phi}_{S,\mathcal{M}}^T \mathbf{R}^{-1} \mathbf{y}_S. \tag{1.35}$$

For an insufficiently measured system, the matrix $\mathbf{\Phi}_{S,\mathcal{M}}^T \mathbf{R}^{-1} \mathbf{\Phi}_{S,\mathcal{M}}$ is a singular matrix. Thus, the addition of the term $\mu \mathbf{L}$ is essential for the numerical stability of the proposed GSP-WLS estimator.

Approach 3. WLS with graph bandlimitness-based regularization: Another GSP approach involves using the bandlimitness assumption in Definition 1.1. Thus, in this case, we formulate the GLP-WLS estimator by incorporating the graph-bandlimitness property in (1.14) as the constraint on the WLS problem in (1.32) as follows:

$$\begin{aligned} \hat{\mathbf{x}}^{GLP-WLS} = \arg \min_{\mathbf{x} \in \mathbb{R}^{|\mathcal{M}|}} & (\mathbf{y}_S - \mathbf{\Phi}_{S,\mathcal{M}}(\mathbf{L})\mathbf{x})^T \mathbf{R}^{-1} (\mathbf{y}_S - \mathbf{\Phi}_{S,\mathcal{M}}(\mathbf{L})\mathbf{x}) \\ & \text{such that } [\mathbf{V}^T \mathbf{x}]_k = 0, \quad k = \beta + 1, \ldots, |\mathcal{M}|, \end{aligned} \tag{1.36}$$

where $\mathbf{V}^T \mathbf{x}$ is the graph spectral representation of $\mathbf{x}$, as defined in (1.11). Due to the constraint in (1.36), the estimated signal, $\hat{\mathbf{x}}^{GLP-WLS}$, obtains nonzero elements only in the graph frequencies $\{\lambda_1, \ldots, \lambda_\beta\}$ that are located in the lower regime of the graph spectrum.

By substituting $\mathbf{x} = \mathbf{I}\mathbf{x} = \mathbf{V}\mathbf{V}^T\mathbf{x}$ in (1.36), denoting $\mathbf{\Theta} \triangleq \mathbf{\Phi}_{S,\mathcal{M}}\mathbf{V}$, and then placing the constraint in the cost function, we obtain the following WLS problem:

$$\begin{aligned} \hat{\tilde{\mathbf{x}}}_{1:\beta}^{GLP-WLS} &= \arg \min_{\tilde{\mathbf{x}}_{1:\beta} \in \mathbb{R}^\beta} (\mathbf{y}_S - \mathbf{\Theta}_{1:\beta} \tilde{\mathbf{x}}_{1:\beta})^T \mathbf{R}^{-1} (\mathbf{y}_S - \mathbf{\Theta}_{1:\beta} \tilde{\mathbf{x}}_{1:\beta}) \\ &= (\mathbf{\Theta}_{1:\beta}^T \mathbf{R}^{-1} \mathbf{\Theta}_{1:\beta})^{-1} \mathbf{\Theta}_{1:\beta} \mathbf{R}^{-1} \mathbf{y}_S, \end{aligned} \tag{1.37}$$

where the submatrix $\mathbf{\Theta}_{1:\beta}$ includes the rows in $\mathbf{\Theta}$ associated with the indices $1, \ldots, \beta$, and $\tilde{\mathbf{x}}_{1:\beta}$ includes the elements of $\tilde{\mathbf{x}}$ in the positions $1, \ldots, \beta$. Now, by setting $\hat{\tilde{\mathbf{x}}}_{\beta+1:|\mathcal{M}|} = \mathbf{0}$, we solve (1.36) by $\hat{\mathbf{x}}^{GLP-WLS} = \mathbf{V}\hat{\tilde{\mathbf{x}}}^{GLP-WLS}$.

1.5.2 GSP-Based Sampling Policies

Managing energy consumption in WSNs is crucial, especially concerning sensing and data forwarding tasks, as they significantly influence node lifespan and network efficiency [Chiumento et al., 2019]. While improving sensor energy efficiency or devising specialized radio protocols can help conserve energy, an equally potent solution involves selective sensing in which sensors are activated only when and where needed. In traditional DSP, downsampling involves reducing the number of samples of a time series. Similarly, in GSP, downsampling refers to sampling a graph signal across a subset of nodes. By incorporating graph topology, additional information on how a signal propagates across vertices can be considered in WSNs. This raises the question: What constitutes a good sampling subset, given

limitations on bandwidth, power, and the number of sensors for the sampled graph signal?

We consider a situation where the WSN operates with constrained sensing resources, possibly due to limitations in energy and communication budgets. In such instances, optimizing sensor placements becomes crucial, and various criteria can guide this optimization process. Existing sampling policies include:

- Task-based sampling in which a sample allocation rule is designed for the sensing model in (1.31) with the goal of minimizing the mean-squared-error (MSE).
- Experimentally designed (E-design) sampling [Chen et al., 2015b] aims to minimize the worst-case errors by maximizing the smallest singular value of the matrix $\mathbf{V}_{\mathcal{S},\mathcal{M}}^T \mathbf{V}_{\mathcal{S},\mathcal{M}}$.
- A-optimal design (A-design) sampling [Chen et al., 2015b] aims to minimize the average errors by seeking $\mathcal{S}$, which minimizes the trace of the matrix inverse $\mathrm{Tr}((\mathbf{V}_{\mathcal{S},\mathcal{M}}^T \mathbf{V}_{\mathcal{S},\mathcal{M}})^{-1})$.
- Cramér–Rao bound (CRB) minimization-based methods have been designed for the general model discussed in (1.31). These methods are based on minimizing the CRBs on the MSE performance (see, e.g. [Dabush et al., 2023; Routtenberg, 2021]).

These sampling policies address the challenge of optimizing sensor placements or selecting a subset of activated sensors under resource constraints in WSNs. The choice among these strategies depends on the specific objectives and criteria relevant to the application scenario, providing flexibility in adapting to different constraints and requirements.

1.6 GSP-Based Anomaly Detection for WSN

Detecting anomalies in WSNs is a critical task. These anomalies often emanate from sensor malfunctions or disruptions in communication links, which may potentially damage hardware and/or affect application performance [Rajasegarar et al., 2008; Xie et al., 2011; Erhan et al., 2021]. Detecting these anomalies is challenging, particularly when dealing with a large number of sensors in the network and/or when anomalies are deliberately concealed.

In this section, we leverage smoothness and GLP signal properties in order to detect anomalies. This approach has been presented in the context of temperature sensors in Sandryhaila and Moura [2014], WSNs in Egilmez and Ortega [2014], and detection of false data injection (FDI) attacks in power systems in Drayer and Routtenberg [2019], Dabush and Routtenberg [2022], and Morgenstern et al. [2024].

1.6.1 Hypothesis Testing Problem

We consider the following hypothesis testing problem:

$$\begin{cases} \mathcal{H}_0: \ \mathbf{z} = \mathbf{x} + \mathbf{n} \\ \mathcal{H}_1: \ \mathbf{z} = \mathbf{x} + \mathbf{a} + \mathbf{n}, \end{cases} \tag{1.38}$$

where the null hypothesis $\mathcal{H}_0$, indicates regular system operations, and $\mathcal{H}_1$, indicates disruptive interference in the system operation. Here, the vector $\mathbf{z}$ represents either sensor readings or their estimates. The system signal, $\mathbf{x}$, is assumed to satisfy local properties w.r.t. the graph. For example, the signal could be smooth, i.e. with a small GTV as defined in (1.12), to be a GLP signal, or even bandlimited graph signal as defined in Definition 1.1. The noise vector $\mathbf{n}$ is considered to be random. The anomaly is modeled by the deterministic vector $\mathbf{a}$, which is an arbitrary vector. Hence, it is not considered smooth, low-pass, or bandlimited w.r.t. the graph.

1.6.2 Graph High-Pass Filter (GHPF)-Based Detection

As mentioned below (1.13), the smooth graph signal, $\mathbf{x}$, can be considered as a GLP signal. Thus, under the assumption that the influence of noise is limited, we can use the following general detector:

$$\left\| h(\mathbf{L})\mathbf{z} \right\|^2 \underset{\mathcal{H}_0}{\overset{\mathcal{H}_1}{\gtrless}} \gamma, \tag{1.39}$$

where γ is the detection threshold determined based on the tested WSN application. Here, $h(\mathbf{L})$ is a graph high-pass filter (GHPF) that preserves the energy at the higher graph frequencies of its input, while reducing the content of the signal at the lower graph frequency regime. This detector is based on the assumption that the anomaly, $\mathbf{a}$, is neither smooth nor small enough to be neglected, and thus, it is expected to obtain energy in the higher graph frequencies. Consequently, it is expected that under $\mathcal{H}_1$, the measurement signal, $\mathbf{z}$, will obtain energy in higher graph frequencies. Thus, as a result, it is expected that the l.h.s. of (1.39) will exceed the threshold under hypothesis $\mathcal{H}_1$.

Examples of GHPFs include the ideal GHPF, which is defined by the graph frequency response

$$h^{id}(\lambda_k) = \begin{cases} 0 & \lambda_k \leq \lambda_{cut} \\ 1 & \lambda_k > \lambda_{cut} \end{cases} \qquad k = 1, \ldots, |\mathcal{M}|, \tag{1.40}$$

where λ_{cut} is the cutoff frequency. Another example is the GTV graph filter, which is defined by $h^{TV}(\mathbf{L}) = \mathbf{L}^{0.5}$. By substituting this graph filter in (1.39), we obtain that for this case the detector is reduced to

$$\|h^{TV}(\mathbf{L})\mathbf{z}\|^2 = \mathbf{z}^T\mathbf{L}^{0.5}\mathbf{L}^{0.5}\mathbf{z} = \mathbf{z}^T\mathbf{L}\mathbf{z}. \tag{1.41}$$

Thus, the GHPF detector in (1.39) is a generalization of the smoothness detector that has been used in Sandryhaila and Moura [2013] and Drayer and Routtenberg [2019].

1.6.3 Illustrative Example

In this example, our goal is to demonstrate the influence of a malfunction in one sensor of a WSN on the measurements of a smooth graph signal. We consider the graph in Figure 1.3b and define the following GLP signal in the graph frequency domain: $\tilde{\mathbf{x}} = \{0.32, 0.28, 0.15, 0.01, 0.01, 0.01, 0, 0, 0, 0\}$. Thus, $\tilde{\mathbf{x}}$ is a GLP signal and a β-bandlimited graph signal, as defined in (1.14), with a cutoff frequency of $\beta = 6$. The signal in the node domain is computed by the inverse GFT in (1.11). We model the anomaly by the additive vector $\mathbf{a} = \{0, 0, 0, 0, -0.3, 0, 0, 0, 0, 0\}$, where an anomaly is inserted at the fifth sensor.

In Figure 1.8, we present the signals $\mathbf{x}$ and $\mathbf{x} + \mathbf{a}$ in both domains. First, it can be seen that the differences between the signals are not clearly evident in the graph

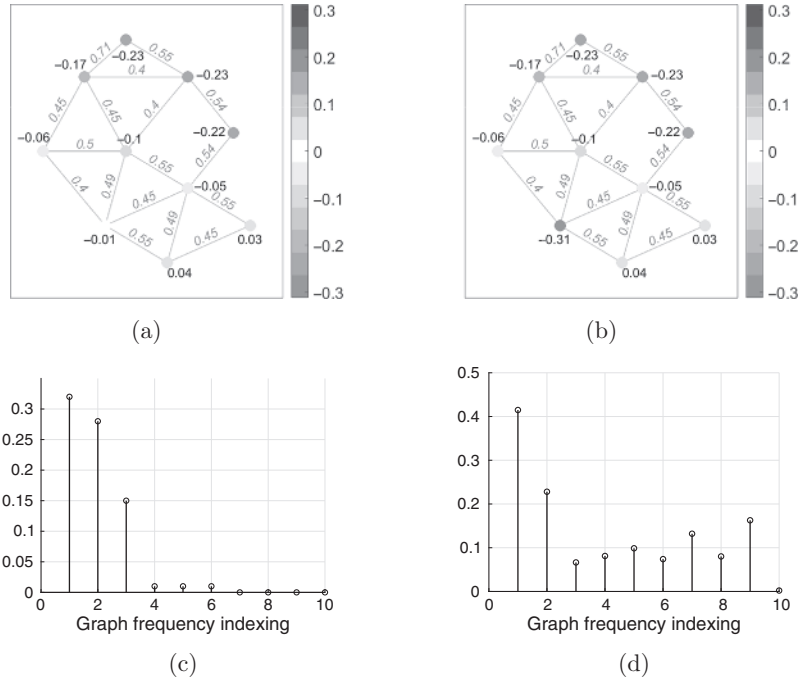

Figure 1.8 Results from the illustrative example in Section 1.6.3 showing the influence of an additive anomaly, $\mathbf{a}$, on a graph signal, $\mathbf{x}$, presented in both the graph node and the graph frequency domains. (a) $\mathbf{x}$, $TV^{\mathcal{G}}(\mathbf{x}) = 0.051$, (b) $\mathbf{x} + \mathbf{a}$, $TV^{\mathcal{G}}(\mathbf{x} + \mathbf{a}) = 0.189$, (c) $\tilde{\mathbf{x}} = \mathbf{V}^T\mathbf{x}$, and (d) $\tilde{\mathbf{x}} + \tilde{\mathbf{a}} = \mathbf{V}^T(\mathbf{x} + \mathbf{a})$.

node domain while the GTVs $TV^{\mathcal{G}}(\mathbf{x}) = 0.0212$ and $TV^{\mathcal{G}}(\mathbf{x} + \mathbf{a}) = 0.2114$ are significantly different. Moreover, the addition of the anomaly results in abnormal energy in the higher graph frequencies. Consequently, the detector in (1.39) is suitable for detecting this anomaly.

1.7 GSP-Based Graph Topology Identification for Modeling WSNs

In Section 1.2, several approaches based on GSP for modeling WSNs are presented. These models rely on prior knowledge of certain factors such as the location of the sensor nodes (i.e. the distance-based model in (1.2)), the correlation between the sensor nodes (i.e. the correlation-based model in (1.3)), or structural data (e.g. transportation networks and power systems). Unfortunately, this prior information may be unavailable or unreliable in some cases. For instance, the exact locations of some of the sensor nodes in a WSN may be unknown [Boukerche et al., 2007]. Additionally, in most cases, the correlation between the sensor nodes in the WSNs is unknown and must be estimated based on data samples [Vuran et al., 2004]. Furthermore, in infrastructure networks, such as power systems, the topology is subject to edge disconnections due to line outages [Shaked and Routtenberg, 2021]. Therefore, there is a need for methods to validate or estimate the underlying interactions in WSNs.

Graph topology inference approaches rely on algebraic and statistical methods. Classic examples include correlation-based methods [Kolaczyk and Csárdi, 2014], Graphical Lasso [Friedman et al., 2008], and GSP-based models [Kalofolias, 2016; Egilmez et al., 2017; Segarra et al., 2017; Medvedovsky et al., 2024]. In this context, GSP-based topology identification is vital for understanding and managing complex systems. Topology identification has applications in diverse fields such as gene regulatory, brain, power, and social networks [Giannakis et al., 2018]. Consequently, using GSP for topology identification in WSNs holds significant promise for enhancing WSN applications.

A key method for topology identification is based on the estimation of the graph Laplacian matrix of the graph, which captures the graph structure and its fundamental qualities. As presented in Sections 1.3–1.6, the graph Laplacian matrix is used in the spectral analysis of graph signals, graph filters, anomaly detection, and signal sampling and recovery, and thus, its accurate estimation is of great importance.

1.7.1 ML Estimation of the Graph Laplacian Matrix

In this section, we derive the general ML estimator under graph Laplacian constraints. These constraints can be implemented by requiring the ML estimator to

belong to the set of Laplacian matrices for connected graphs, which can be defined as [Ying et al., 2020b]

$$\mathcal{L} = \left\{ \mathbf{L} \in \mathcal{S}_+^p \mid \mathrm{L}_{k,m} \leq 0, \forall\, k \neq m, \mathbf{L1} = \mathbf{0}, \mathrm{rank}(\mathbf{L}) = |\mathcal{M}| \right\}. \tag{1.42}$$

where $\mathcal{S}_+^p$ is the set of $p \times p$ symmetric positive semi-definite matrices. The graph estimation problem is approached by formulating it as a Laplacian learning problem based on a probabilistic graphical model [Banerjee et al., 2008; Koller and Friedman, 2009]. Thus, we assume that we have i.i.d. data samples, $\mathbf{x}_1, \ldots, \mathbf{x}_n$, drawn from a zero-mean Gaussian distribution parametrized by a positive semi-definite precision matrix, $\mathbf{L}$, i.e. $\mathbf{x} \sim \mathcal{N}(\mathbf{0}, \mathbf{L}^\dagger)$. This defines an improper Laplacian-constrained Gaussian Markov Random Field (LGMRF) model. The ML estimator of $\mathbf{L}$ under this model can be obtained by solving the following constrained minimization of the negative log-likelihood:

$$\hat{\mathbf{L}}^{ML} = \arg \min_{\mathbf{L} \in \mathcal{L}} \left\{ Tr(\mathbf{LS}) - \log |\mathbf{L}|_+ \right\}, \tag{1.43}$$

where $\mathbf{S} \triangleq \frac{1}{n} \sum_{i=1}^n \mathbf{x}_i \mathbf{x}_i^T$ is the sample covariance matrix, $Tr(\cdot)$ denotes the trace operator, and $(\cdot)_+$ denotes the pseudo-determinant. It should be noted that various objective functions can be considered for topology identification under different assumed models within the constrained setting of $\mathbf{L} \in \mathcal{L}$. For example, in [Grotas et al, 2019] and [Halihal and Routtenberg, 2022], the topology of a power system is identified by solving the ML estimator of the Laplacian-constrained setting, where the samples are modeled using power flow equations.

Sparsity, which plays an important role in high-dimensional learning, can also be incorporated into the problem in (1.43). A sparse graph estimation problem under the LGMRF model can be formulated by adding a sparse penalty function to the estimator in (1.43). Specifically, selecting the penalty function as $|\mathbf{L}|_{1,\mathrm{off}} = \sum_{k \neq m} |L_{k,m}|$ yields the same objective function as the well-known Graphical Lasso problem. However, due to the Laplacian constraints in (1.43), this penalty function is ineffective [Ying et al., 2020a]. Alternative approaches utilizing nonconvex penalties have been proposed to address this issue, as discussed in Medvedovsky et al. [2024]. This result highlights the fact that Laplacian-based GSP approaches are not merely straightforward extensions of conventional methods, but require careful consideration.

1.7.2 Topology Change Identification

Dynamic topology estimation, especially in WSNs with limited cooperation, presents unique challenges. Advances such as those already in 5G technology and those expected in 6G technology [Xia et al., 2020; Yeh et al., 2023] are making WSNs increasingly crucial in many aspects, and understanding their structure

has become a significant concern. A critical application is in the security context, where comprehending the structure of adversary communication networks is of paramount importance. Traditional methods, typically designed for static, unchanging network structures, fall short in addressing the complexities of these modern dynamic environments. In this section, we discuss the application of detecting changes in the topology within dynamic settings.

Specifically, we consider the problem of identifying the underlying graph associated with a set of smooth graph signals $\{\mathbf{y}[n]\}_{n=1}^{N}$, obtained as outputs of a smooth graph filter as defined in (1.22). The underlying graph can be either the original graph, denoted as $\mathcal{G}^0 = (\mathcal{M}, \xi^0)$, or any graph from the set $\{\mathcal{G}^d = (\mathcal{M}, \xi^d)\}_{d=1}^{D}$ that is obtained by disconnecting a set $\mathcal{C}^d$ of edges from the original graph. This problem is formulated in the following multiple hypothesis testing problem:

$$\begin{cases} \mathcal{H}_0 : \mathbf{y}[n] = h(\mathbf{L}^{(0)})\mathbf{x}[n] \\ \mathcal{H}_d : \mathbf{y}[n] = h(\mathbf{L}^{(d)})\mathbf{x}[n], \quad n = 1, \dots, N, \end{cases} \tag{1.44}$$

for $d = 1, \dots, D$, where under each hypothesis $\mathcal{H}_d$, $d = 0, \dots, D$, the graph filter $h(\mathbf{L}^{(d)})$ is a smooth graph filter as in (1.20). Additionally, in each of the hypothesis $\mathcal{H}_d, d = 1, \dots, D$, the graph Laplacian matrix is given by

$$\mathbf{L}^{(d)} = \mathbf{L}^{(0)} + \mathbf{E}^d, \qquad \mathbf{E}^d = \sum_{(i,j)\in\mathcal{C}^{(d)}} \mathbf{E}^{(i,j)}, \tag{1.45}$$

where the addition of $\mathbf{E}^{(i,j)}$ to the graph Laplacian matrix models the removal of the edge (i, j) from the graph. The signal-edge disconnection matrix $\mathbf{E}^{(i,j)}$ is defined elementwisely by

$$E_{k,m}^{(i,j)} = L_{k,m}^{(0)} \times \begin{cases} -1 & \{k = m = i\} \cup \{k = m = j\} \\ 1 & \{k = i, m = j\} \cup \{k = j, m = i\} \\ 0 & \text{otherwise.} \end{cases} \tag{1.46}$$

For the sake of simplicity, we assume that under each alternative hypothesis $\mathcal{H}_d$, the graph filter that is used to generate the measurements is a non-singular matrix, and the eigenvalues of the graph Laplacian matrix are distinct. In addition, we assume that $\mathbf{x}[n] \overset{i.i.d.}{\sim} \mathcal{N}(\mathbf{0}, \mathbf{I})$. While these assumptions are chosen for simplicity, the problem in (1.44) can be solved without these assumptions, as shown in [Shaked and Routtenberg, 2021].

We solve the multiple hypothesis testing problem in (1.44) with the ML decision rule [Kay, 1993b]:

$$\begin{aligned} \hat{d} &= \arg\max_{0\le d\le D} \log f(\mathbf{y}; \mathbf{L}^{(d)}) \\ &= \arg\max_{0\le d\le D} -\frac{1}{2}\sum_{n=1}^{N} \mathbf{y}^T[n](h^2(\mathbf{L}^{(d)}))^{-1}\mathbf{y}[n] + \log(|h^2(\mathbf{L}^{(d)})|), \end{aligned} \tag{1.47}$$

where $\log(f(\mathbf{y};\mathbf{L}^{(d)}))$ are the log-likelihoods under each hypothesis $\mathcal{H}_d$, $d = 0,\dots,D$. The last equality results from substituting the distribution of the smooth output graph signal $\mathbf{y}[n] \overset{i.i.d.}{\sim} \mathcal{N}(\mathbf{0}, h^2(\mathbf{L}^{(d)}))$ in the log-likelihood function, and then removing constant terms.

In order to analyze the result in (1.47) in the graph frequency domain, based on (1.10) and (1.15), we use the notation $\{\lambda_1^{(d)} \dots \lambda_{|\mathcal{M}|}^{(d)}\}$, $\mathbf{V}^{(d)}$, and $\{h(\lambda_1^{(d)}),\dots,h(\lambda_{|\mathcal{M}|}^{(d)})\}$ for the graph frequencies, eigenvectors, and graph filter response, associated with the graph Laplacian matrix $\mathbf{L}^{(d)}$. In [Shaked and Routtenberg, 2021], it was shown that (1.47) can be written as

$$\hat{d} = \arg\max_{0\le d\le D} -\frac{1}{2}\sum_{k=1}^{|\mathcal{M}|}(h^2(\lambda_k^{(d)}))^{-1}\sum_{n=1}^{N}(\tilde{y}_k^{(d)})^2[n] + \sum_{k=1}^{|\mathcal{M}|}\log\ h^2(\lambda_k^{(d)}), \tag{1.48}$$

where the kth element of the mean-squared GFT of the output graph signal is defined as

$$\psi_k^{(d)} \triangleq \frac{1}{|\mathcal{M}|}\sum_{n=1}^{N}(\tilde{y}_k^{(d)})^2[n]. \tag{1.49}$$

By substituting (1.49) with (1.48), we obtain

$$\hat{d} = \arg\max_{0\le d\le D} -\sum_{k=1}^{|\mathcal{M}|}\frac{\psi_k^{(d)}}{h^2(\lambda_k^{(d)})} + \sum_{k=1}^{|\mathcal{M}|}\log\ h^2(\lambda_k^{(d)}). \tag{1.50}$$

It can be seen from (1.50) that sufficient statistics for the ML decision rule are the graph frequency energy levels $\{\psi_k^{(d)}\}_{k=1}^{|\mathcal{M}|}$, $d = 0,\dots,D$. Additionally, for smooth graph filters, as defined in Definition 1.4, the weights of the graph frequency levels in (1.50), $(1/h^2(\lambda_k^{(d)}))$, amplify the influence of low graph-frequencies. Therefore, the ML decision rule is governed by the low-graph frequencies, which can be associated with the graph signal smoothness property.

1.8 Conclusions and Future Directions

In this chapter, we have outlined the fundamentals of GSP and showcased an end-to-end GSP-based approach for signal processing in WSN applications. In Section 1.2, we discussed the modeling of WSNs as undirected weighted graphs and presented several models that consider features such as the distance and correlation between the sensor nodes. In Section 1.3, we outlined fundamental concepts in GSP, including graph signals, graph filters, graph signal properties (e.g. graph signal smoothness), and graph spectral analysis. We then expanded upon graph signal smoothness in Section 1.4. Specifically, we introduced the concept of smooth graph filters, formulated a composite hypothesis testing problem differentiating between outputs of smooth or non-smooth graph filters, and

derived a semi-parametric detector that solves this composite testing problem. Then, we utilized the graph signal smoothness property for practical applications in WSNs. In Section 1.5, we derived an ML-based estimator for signal recovery in models with missing data. In Section 1.6, we used graph signal smoothness for anomaly detection. Finally, in Section 1.7, we presented approaches for identifying the topology of the WSN underlying graph.

The exploration of GSP within the context of WSNs has unveiled significant insights into the effectiveness of GSP-based tools for the analysis and manipulation of WSN data. As we chart the course for future directions, several promising avenues merit attention. First, in addition to GSP, the advent of GNNs is expected to provide useful tools for modeling intricate graph-structured data. Future research should delve into synergies between GSP and GNNs to enhance the understanding and processing capabilities of WSN data. Additionally, investigating the synergy between GSP and the deployment of WSNs could lead to optimized network architectures that leverage the inherent strengths of both. Their considerations should incorporate practical aspects such as network layers and physical attributes, including capacity and coverage. Specifically, utilizing GSP for clustering within WSNs holds the potential to reveal hidden patterns and improve overall network efficiency. Furthermore, to address inherent limitations on energy resources, processing power, communication constraints, and computational costs [Egilmez and Ortega, 2014], it is crucial to develop distributed GSP techniques to minimize communication costs, enhance energy and processing efficiency, and adhere to the physical constraints of the system. Moreover, as the field of GSP grows, it is becoming clear that methods for identifying topologies need to be flexible in order to develop robust and efficient communication systems. Thus, incorporating GSP tools for this task may enable a better understanding of the underlying network structure promoting better decision-making in WSN applications. Finally, the analysis of specific structures inherent in typical WSN networks, such as the star topology, hierarchical/tree topology, and mesh topology (see Figure 1.9), may lay the basis to develop tailored GSP techniques for optimized performance for diverse WSN architectures. In essence, the integration of GSP into WSN research opens up a spectrum of possibilities,

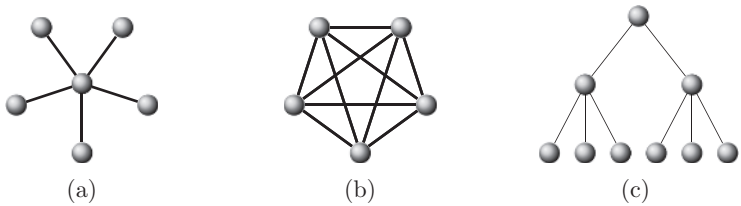

Figure 1.9 Network topologies. (a) Star, (b) Mesh, and (c) Tree.

and these future directions can further enhance the synergy between GSP and WSNs, thereby advancing the capabilities and applications of this dynamic field.

Acknowledgments

This work is partially supported by the Israel Science Foundation (Grant no. 1148/22), the Jabotinsky Scholarship from the Israel Ministry of Technology and Science, the Israel Ministry of National Infrastructure and Energy, and the US National Science Foundation under Grants CNS-2128448 and ECCS-2335876.

Bibliography

I. F. Akyildiz, W. Su, V. Sankarasubramaniam, and E. Cayirci. Wireless sensor networks: A survey. *Computer Networks*, 38(4):393–422, 2002.

O. Banerjee, L. El Ghaoui, and A. d'Aspremont. Model selection through sparse maximum likelihood estimation for multivariate Gaussian or binary data. *The Journal of Machine Learning Research*, 9:485–516, 2008.

M. Belkin, I. Matveeva, and P. Niyogi. Regularization and semi-supervised learning on large graphs. In *Proceedings of the 17th Annual Conference on Learning Theory*, pages 624–638. Springer, 2004.

A. Boukerche, H. A. Oliveira, E. F. Nakamura, and A. Loureiro. Localization systems for wireless sensor networks. *IEEE Wireless Communications*, 14(6):6–12, 2007.

D. Cai, X. He, J. Han, and T. S. Huang. Graph regularized nonnegative matrix factorization for data representation. *IEEE Transactions on Pattern Analysis and Machine Intelligence*, 33(8):1548–1560, 2010.

M. Cardei, Y. Yang, and J. Wu. Non-uniform sensor deployment in mobile wireless sensor networks. In *Proceedings of the IEEE International Symposium on a World of Wireless, Mobile and Multimedia Networks*, pages 1–8, 2008.

S. Chen, A. Sandryhaila, J. M. F. Moura, and J. Kovačević. Signal recovery on graphs: Variation minimization. *IEEE Transactions on Signal Processing*, 63(17):4609–4624, 2015a.

S. Chen, R. Varma, A. Sandryhaila, and J. Kovačević. Discrete signal processing on graphs: Sampling theory. *IEEE Transactions on Signal Processing*, 63(24):6510–6523, 2015b.

A. Chiumento, N. Marchetti, and I. Macaluso. Energy efficient WSN: A cross-layer graph signal processing solution to information redundancy. In *Proceeding of the International Symposium on Wireless Communication Systems (ISWCS)*, pages 645–650. IEEE, 2019.

L. Dabush and T. Routtenberg. Detection of false data injection attacks in unobservable power systems by Laplacian regularization. In *Proceedings of the Sensor Array and Multichannel Signal Processing Workshop (SAM)*, pages 415–419, 2022.

L. Dabush and T. Routtenberg. "Verifying the Smoothness of Graph Signals: A Graph Signal Processing Approach," in *IEEE Transactions on Signal Processing*, vol. 72, pp. 4349–4365, 2024, doi: 10.1109/TSP.2024.3439554.

L. Dabush, A. Kroizer, and T. Routtenberg. State estimation in partially observable power systems via graph signal processing tools. *Sensors*, 23(3):1387, 2023.

S. E. Díaz, J. C. Pérez, A. C. Mateos, M. C. Marinescu, and B. B. Guerra. A novel methodology for the monitoring of the agricultural production process based on wireless sensor networks. *Computers and Electronics in Agriculture*, 76(2):252–265, 2011.

X. Dong, D. Thanou, L. Toni, M. Bronstein, and P. Frossard. Graph signal processing for machine learning: A review and new perspectives. *IEEE Signal Processing Magazine*, 37(6):117–127, 2020.

E. Drayer and T. Routtenberg. Detection of false data injection attacks in smart grids based on graph signal processing. *IEEE Systems Journal*, 14(2):1886–1896, 2019.

H. E. Egilmez and A. Ortega. Spectral anomaly detection using graph-based filtering for wireless sensor networks. In *Proceedings of the IEEE International Conference on Acoustics, Speech and Signal Processing (ICASSP)*, pages 1085–1089, 2014.

H. E. Egilmez, E. Pavez, and A. Ortega. Graph learning from data under Laplacian and structural constraints. *IEEE Journal on Selected Topics in Signal Processing*, 11(6):825–841, 2017.

A. Elmoataz, O. Lezoray, and S. Bougleux. Nonlocal discrete regularization on weighted graphs: A framework for image and manifold processing. *IEEE Transactions on Image Processing*, 17(7):1047–1060, 2008.

L. Erhan, M. Ndubuaku, M. D. Mauro, W. Song, M. Chen, G. Fortino, O. Bagdasar, and A. Liotta. Smart anomaly detection in sensor systems: A multi-perspective review. *Information Fusion*, 67:64–79, 2021.

J. Feng, F. Chen, and H. Chen. Data reconstruction coverage based on graph signal processing for wireless sensor networks. *IEEE Wireless Communications Letters*, 11(1):48–52, 2021.

J. Friedman, T. Hastie, and R. Tibshirani. Sparse inverse covariance estimation with the graphical lasso. *Biostatistics*, 9(3):432–441, 2008.

G. B. Giannakis, Y. Shen, and G. V. Karanikolas. Topology identification and learning over graphs: Accounting for nonlinearities and dynamics. *Proceedings of the IEEE*, 106(5):787–807, 2018.

S. Grotas, Y. Yakoby, I. Gera, and T. Routtenberg. Power systems topology and state estimation by graph blind source separation. *IEEE Transactions on Signal Processing*, 67(8):2036–2051, 2019.

M. Halihal and T. Routtenberg. Estimation of the admittance matrix in power systems under Laplacian and physical constraints. In *Proceeding of the IEEE International Conference on Acoustics, Speech and Signal Processing (ICASSP)*, pages 5972–5976, 2022.

E. Hasheminejad and H. Barati. A reliable tree-based data aggregation method in wireless sensor networks. *Peer-to-Peer Networking and Applications*, 14(2):873–887, 2021.

Y. He and H. T. Wai. Detecting central nodes from low-rank excited graph signals via structured factor analysis. *IEEE Transactions on Signal Processing*, 70:2416–2430, 2022.

T. He, S. Krishnamurthy, J. A. Stankovic, T. Abdelzaher, L. Luo, R. Stoleru, T. Yan, L. Gu, J. Hui, and B. Krogh. Energy-efficient surveillance system using wireless sensor networks. In *Proceedings of the International Conference on Mobile Systems, Applications, and Services*, pages 270–283, 2004.

E. Isufi, F. Gama, D. I. Shuman and S. Segarra. "Graph Filters for Signal Processing and Machine Learning on Graphs," in *IEEE Transactions on Signal Processing*, vol. 72, pp. 4745–4781, 2024. doi: 10.1109/TSP.2024.3349788.

V. Kalofolias. How to learn a graph from smooth signals. In *Artificial Intelligence and Statistics (PMLR)*, pages 920–929, 2016.

D. Kandris, C. Nakas, D. Vomvas, and G. Koulouras. Applications of wireless sensor networks: An up-to-date survey. *Applied System Innovation*, 3(1):14, 2020.

S. M. Kay. *Fundamentals of Statistical Signal Processing: Estimation Theory*, volume 1. Prentice Hall PTR, New Jersey, NJ, USA, 1993a.

S. M. Kay. *Fundamentals of Statistical Signal Processing, Volume II: Detection Theory*. Prentice Hall PTR, New Jersey, NJ, USA, 1993b.

B. S. Kim, K. I. Kim, B. Shah, F. Chow, and K. H. Kim. Wireless sensor networks for big data systems. *Sensors*, 19(7):1565, 2019.

E. D. Kolaczyk and G. Csárdi. *Statistical Analysis of Network Data with R*, volume 65. Springer, Cham, Switzerland, 2014.

D. Koller and N. Friedman. *Probabilistic Graphical Models: Principles and Techniques*. MIT Press, Massachusetts, MA, USA, 2009.

L. Kong, M. Xia, X. Y. Liu, G. Chen, Y. Gu, M. Y. Wu, and X. Liu. Data loss and reconstruction in wireless sensor networks. *IEEE Transactions on Parallel and Distributed Systems*, 25(11):2818–2828, 2013.

A. Kroizer, T. Routtenberg, and Y. C. Eldar. Bayesian estimation of graph signals. *IEEE Transactions on Signal Processing*, 70:2207–2223, 2022.

Y. Li and L. E. Parker. A spatial-temporal imputation technique for classification with missing data in a wireless sensor network. In *Proceedings of the International Conference on Intelligent Robots and Systems*, pages 3272–3279, 2008.

A. G. Marques, S. Segarra, G. Leus, and A. Ribeiro. Sampling of graph signals with successive local aggregations. *IEEE Transactions on Signal Processing*, 64(7):1832–1843, 2015.

Y. Medvedovsky, E. Treister, and S. T. Routtenberg. Efficient Graph Laplacian Estimation by Proximal Newton. Proceedings of The 27th International Conference on Artificial Intelligence and Statistics, *Proceedings of Machine Learning Research*, 238:1171–1179, 2024. Available from https://proceedings.mlr.press/v238/medvedovsky24a.html.

G. Morgenstern and T. Routtenberg (2024). "Efficient Recovery of Sparse Graph Signals From Graph Filter Outputs," in *IEEE Transactions on Signal Processing*, vol. 72, pp. 5550–5566. doi: 10.1109/TSP.2024.3495225.

G. Morgenstern, J. Kim, J. Anderson, G. Zussman, and T. Routtenberg. Protection against graph-based false data injection attacks on power systems. *IEEE Transactions on Control of Network Systems*, 11(4):1924–1936, 2024.

Z. Nurlan, T. Zhukabayeva, M. Othman, A. Adamova, and N. Zhakiyev. Wireless sensor network as a mesh: Vision and challenges. *IEEE Access*, 10:46–67, 2021.

A. Ortega. *Introduction to Graph Signal Processing*. Cambridge University Press, 2022.

A. Ortega, P. Frossard, J. Kovačević, J. M. F. Moura, and P. Vandergheynst. Graph signal processing: Overview, challenges, and applications. *Proceedings of the IEEE*, 106(5):808–828, 2018.

L. Pan and J. Li. K-nearest neighbor based missing data estimation algorithm in wireless sensor networks. *Wireless Sensor Network*, 2(02):115, 2010.

S. Pattem, B. Krishnamachari, and R. Govindan. The impact of spatial correlation on routing with compression in wireless sensor networks. *ACM Transactions on Sensor Networks*, 4(4):1–33, 2008.

S. S. Pradhan, J. Kusuma, and K. Ramchandran. Distributed compression in a dense microsensor network. *IEEE Signal Processing Magazine*, 19(2):51–60, 2002.

G. Puy and P. Pérez. Structured sampling and fast reconstruction of smooth graph signals. *Information and Inference: A Journal of the IMA*, 7(4):657–688, 2018.

S. Rajasegarar, C. Leckie, and M. Palaniswami. Anomaly detection in wireless sensor networks. *IEEE Wireless Communications*, 15(4):34–40, 2008.

R. Ramakrishna, H. T. Wai, and A. Scaglione. A user guide to low-pass graph signal processing and its applications: Tools and applications. *IEEE Signal Processing Magazine*, 37(6):74–85, 2020.

A. Ramamoorthy, J. Shi, and R. D. Wesel. On the capacity of network coding for random networks. *IEEE Transactions on Information Theory*, 51(8):2878–2885, 2005.

D. Romero, M. Ma, and G. B. Giannakis. Kernel-based reconstruction of graph signals. *IEEE Transactions on Signal Processing*, 65(3):764–778, 2016.

T. Routtenberg. Non-Bayesian estimation framework for signal recovery on graphs. *IEEE Transactions on Signal Processing*, 69:1169–1184, 2021.

T. Sahai, A. Speranzon, and A. Banaszuk. Hearing the clusters of a graph: A distributed algorithm. *Automatica*, 48(1):15–24, 2012.

A. Sandryhaila and J. M. F. Moura. Discrete signal processing on graphs. *IEEE Transactions on Signal Processing*, 61(7):1644–1656, 2013.

A. Sandryhaila and J. M. F. Moura. Discrete signal processing on graphs: Frequency analysis. *IEEE Transactions on Signal Processing*, 62(12):3042–3054, 2014.

A. Sandryhaila, S. Kar, and J. M. F. Moura. Finite-time distributed consensus through graph filters. In *Proceedings of the IEEE International Conference on Acoustics, Speech and Signal Processing (ICASSP)*, pages 1080–1084, 2014.

I. D. Schizas, A. Ribeiro, and G. B. Giannakis. Consensus in Ad Hoc WSNs with noisy links—Part I: Distributed estimation of deterministic signals. *IEEE Transactions on Signal Processing*, 56(1):350–364, 2008.

K. Schultz, A. Saksena, E. P. Reilly, R. Hingorani, and M. Villafae-Delgado. Detecting anomalous swarming agents with graph signal processing. In *Proceedings of the IEEE International Conference on Autonomous Systems (ICAS)*, pages 1–5, 2021.

S. Segarra, A. G. Marques, G. Mateos, and A. Ribeiro. Network topology inference from spectral templates. *IEEE Transactions on Signal and Information Processing Over Networks*, 3(3):467–483, 2017.

S. D. Servetto and G. Barrenechea. Constrained random walks on random graphs: Routing algorithms for large scale wireless sensor networks. In *Proceedings of the ACM International Workshop on Wireless Sensor Networks and Applications*, pages 12–21, 2002.

S. Shaked and T. Routtenberg. Identification of edge disconnections in networks based on graph filter outputs. *IEEE Transactions on Signal and Information Processing Over Networks*, 7:578–594, 2021.

D. I. Shuman, P. Vandergheynst, and P. Frossard. Chebyshev polynomial approximation for distributed signal processing. In *Proceedings of the IEEE International Conference on Distributed Computing in Sensor Systems and Workshops (DCOSS)*, pages 1–8, 2011.

D. I. Shuman, S. K. Narang, P. Frossard, A. Ortega, and P. Vandergheynst. The emerging field of signal processing on graphs: Extending high-dimensional data analysis to networks and other irregular domains. *IEEE Signal Processing Magazine*, 30(3):83–98, 2013.

M. Tariq and H. V. Poor. Real time electricity theft detection in microgrids through wireless sensor networks. 2016 *IEEE Sensors*, pages 1–3, Orlando, FL, USA, 2016. doi: 10.1109/ICSENS.2016.7808729.

M. C. Vuran and I. F. Akyildiz. Spatial correlation-based collaborative medium access control in wireless sensor networks. *IEEE/ACM Transactions On Networking*, 14(2):316–329, 2006.

M. C. Vuran, O. B. Akan, and I. F. Akyildiz. Spatio-temporal correlation: Theory and applications for wireless sensor networks. *Computer Networks*, 45(3):245–259, 2004.

F. Wang and C. Zhang. Label propagation through linear neighborhoods. In *Proceedings of the International Conference on Machine Learning*, pages 985–992, 2006.

G. Werner-Allen, K. Lorincz, J. Johnson, J. Lees, and M. Welsh. Fidelity and yield in a volcano monitoring sensor network. In *Proceedings of the 7th Symposium on Operating Systems Design and Implementation*, pages 381–*396*, 2006.

W. N. V. Wieringen. Lecture notes on ridge regression. *arXiv preprint: 1509.09169*, 2015.

T. Xia, M. M. Wang, J. Zhang, and L. Wang. Maritime internet of things: Challenges and solutions. *IEEE Wireless Communications*, 27(2):188–196, 2020.

M. Xie, S. Han, B. Tian, and S. Parvin. Anomaly detection in wireless sensor networks: A survey. *Journal of Network and Computer Applications*, 34(4):1302–1325, 2011.

C. Yeh, G. Do Jo, Y. J. Ko, and H. K. Chung. Perspectives on 6G wireless communications. *ICT Express*, 9(1):82–91, 2023.

J. Ying, J. V. D M. Cardoso, and D. P. Palomar. Does the ℓ_1-norm learn a sparse graph under Laplacian constrained graphical models? *arXiv preprint: 2006.14925*, 2020a.

J. Ying, J. V. D. M. Cardoso, and D. Palomar. Nonconvex sparse graph learning under Laplacian constrained graphical model. *Advances in Neural Information Processing Systems*, 33:7101–7113, 2020b.

M. Zheng, J. Bu, C. Chen, C. Wang, L. Zhang, G. Qiu, and D. Cai. Graph regularized sparse coding for image representation. *IEEE Transactions on Image Processing*, 20(5):1327–1336, 2010.